N94-11404

Radiation Effects in $Ga_{0.47}In_{0.53}As$ Solar Cells

R.J. Walters, G.J. Shaw*, and G.P. Summers
Naval Research Laboratory, Washington, DC 20375
* G.J. Shaw is supported by the ONT post doctoral fellowship program

S.R. Messenger
SFA, Inc., Landover, MD 20785

ABSTRACT

The effects of irradiating $Ga_{0.47}In_{0.53}As$ p-i-n junctions with 1 MeV electrons have been measured using Deep Level Transient Spectroscopy, (DLTS) and both dark and illuminated (1 sun, air mass zero (AM0)) current-voltage (I-V) measurements. The I-V measurements were made over the range 100K < T < 350K. Temperature coefficients of the $Ga_{0.47}In_{0.53}As$ photovoltaic parameters are presented which follow the same general behavior as other solar cell materials (e.g. Si and GaAs). Fits of the dark I-V data to the two term diode equation before irradiation were satisfactory, yielding an estimated band-gap energy of 0.79 eV. The recombination component of the dark current was found to increase linearly with fluence. DLTS detected two radiation-induced defect levels, one shallow (E_c-0.10 eV) and one near mid-gap (E_c-0.29 eV), and it is the near mid-gap level which is expected to be the cause of the dark current increase. The radiation-induced degradation of the open circuit voltage is shown to be accurately predicted from the dark I-V measurements. The degradation of the open circuit voltage dominated the radiation response of the photovoltaic parameters while the short circuit current was only moderately degraded. This behavior is qualitatively explained in terms of the base thickness and dopant level. Appropriate changes in the device structure are suggested which should increase the radiation resistance. Isochronal thermal annealing induced recovery in the photovoltaic parameters at $\approx$ 400 K, coinciding with an annealing stage of the near mid-gap defect level.

INTRODUCTION

The radiation resistance of InP solar cells is well known to this community. Equally well known are the rapid advance made by the National Renewable Energy Laboratory (NREL) in growing a high efficiency, monolithic $InP/Ga_{0.47}In_{0.53}As$ tandem solar cell [ref 1-3] (figure 1). This cell has achieved efficiencies of 31.8% under 50 suns concentration (direct, 25°C) which was the first time that a monolithic tandem had exceeded 30% efficiency. Under 1 sun, AM0 conditions, this cell has achieved efficiencies of 23.9% (25°C). It has been generally accepted that a multi-band-gap cell with efficiencies of 24% is a viable technology for space power. Clearly, this proves the $InP/Ga_{0.47}In_{0.53}As$ tandem cell to be one of the most efficient photovoltaic power sources available. Because of this, the Naval Research Laboratory (NRL) is participating in an interagency research contract with NREL to develop the $InP/Ga_{0.47}In_{0.53}As$ tandem into a radiation resistant, high efficiency space power source. The financial support for this research is provided in part by the Office of Naval Research.

While the $InP/Ga_{0.47}In_{0.53}As$ tandem cell has demonstrated a beginning of life (BOL) power output which is satisfactory for a space power system, its radiation resistance must be optimized to fully space qualify the cell. The NRL research is designed to do this. As shown at the last InP and Related Materials Conference (April 1992), the top cell of the $InP/Ga_{0.47}In_{0.53}As$ tandem displays a radiation resistance as high as that of the Spire InP homojunctions [4]. However, the radiation response of the $Ga_{0.47}In_{0.53}As$ bottom cell still needs investigation. This paper reports continuing results of 1 MeV electron irradiation of $Ga_{0.47}In_{0.53}As$.

While this study concerns the $Ga_{0.47}In_{0.53}As$ bottom cell, not enough of these devices were immediately available to conduct a full radiation study. Therefore, commercially available $Ga_{0.47}In_{0.53}As$ photodetectors were used as solar cells (fig. 2). It is the radiation response of these devices which is presented here. It is important to note that while the photodetectors are reasonable representations of a $Ga_{0.47}In_{0.53}As$ solar cell, they represent only a single

possible device structure. In particular, the dopant density in the base is an order of magnitude less than the present design of the tandem cell. In this way, the present data is providing information on the dependence of the radiation response on the device structure. This data will be used ultimately to design the $Ga_{0.47}In_{0.53}As$ bottom cell for maximum radiation tolerance. Therefore, the radiation resistance of the $Ga_{0.47}In_{0.53}As$ bottom cell will be higher than that of the photodetectors measured presently.

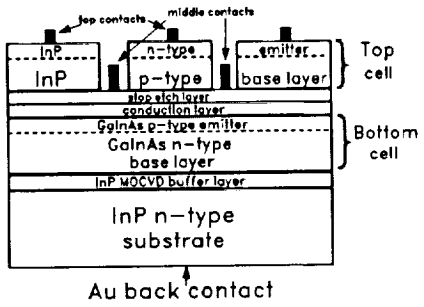

Figure 1: Schematic drawing of the $InP/Ga_{0.47}In_{0.53}As$ tandem solar cell

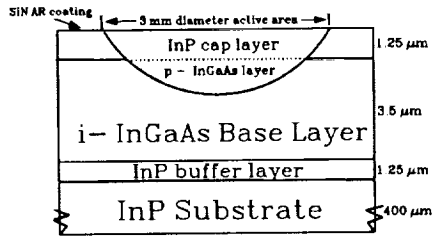

Figure 2: Schematic drawing of the $Ga_{0.47}In_{0.53}As$ photodetector

EXPERIMENTAL NOTES

Results of three different types of measurements are presented- deep level transient spectroscopy (DLTS), current-voltage (I-V) measurements in the dark, and I-V measurements under simulated solar illumination. The DLTS measurements were made using a Bio-Rad DL4600 spectrometer with both liquid nitrogen and liquid helium cooled cryostats. The temperature ranged from 30 to 300 K. A 1 ms fill pulse was used for the DLTS measurements, which was sufficient to saturate the DLTS signal. A reverse bias of -2 V was used. The forward bias was zero volts. Attempts to detect minority charge carrier trapping centers were made by applying a positive fill pulse and by using laser excitation, but no minority carrier traps were detected.

I-V measurements were made with the sample mounted in the DLTS cryostat which allowed measurements throughout the temperature range 100 to 350 K. The liquid nitrogen cryostat is equipped with a sapphire window to allow for illumination of the sample. To simulate space conditions, an AM0 filter was used on the solar simulator adjusted to 1 sun intensity using a standard $InP/Ga_{0.47}In_{0.53}As$ tandem cell calibrated by the NREL. The simulator is an Oriel, 1000 W, xenon arc lamp, portable solar simulator.

The $Ga_{0.47}In_{0.53}As$ photodetectors (fig 2) were grown by Epitaxx Inc. part number EPX-3000CR. The devices were p-i-n structures grown by metalorganic vapor deposition (MOCVD) on n-type InP wafers. The $Ga_{0.47}In_{0.53}As$ base layer had a graded carrier concentration profile (determined here by capacitance-voltage measurements). The concentration ranged from 2×10^{15} cm^{-3} at the junction to about 6×10^{15} cm^{-3} at the substrate. The entire device was capped by 1.25 μm InP layer. The p^+ emitter was formed by thermally diffusing Zn through the InP cap into the $Ga_{0.47}In_{0.53}As$ base. The active area was 7.07 mm^2. A SiN antireflective coating was applied.

RESULTS

A. Dark I-V Measurements

Dark I-V measurements were performed before and after each irradiation step. These measurements were used to determine the initial quality of the junctions and to investigate the important contributions to the junction current. The forward bias dark I-V behavior of a semiconductor junction can be described by [ref 5]

$$I_F = I_{01}\left(e^{qV/k_BT} - 1\right) + I_{02}\left(e^{qV/2k_BT} - 1\right) + \frac{V}{R_{sh}} \qquad (1)$$

where R_{sh} is the diode shunt resistance. The first term on the right hand side describes the diffusion current while

the second term describes the recombination current. For an abrupt p^+n junction containing a single level recombination center located near the middle of the bandgap, the parameters I_{01} and I_{02} have the values [ref 6]:

$$I_{01} = qA\sqrt{\frac{D_p}{\tau_p}}\frac{n_i^2}{N_D} \quad (2)$$

$$I_{02} = \frac{qWA}{2}\sigma v_{th} N_t n_i \quad (3)$$

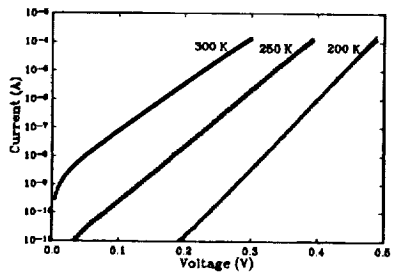

Figure 3: Dark I-V data measured on the $Ga_{0.47}In_{0.53}As$ photodetectors before irradiation. The solid lines are the calculated fits to the data.

In the expression for I_{01} (eq.(2)) D_p and τ_p are the diffusion coefficient and the minority carrier lifetime in the n-type material, respectively. The quantities n_i and N_D are the intrinsic carrier concentration and the doping level, respectively. The expression for I_{02} contains the characteristics of the recombination centers in the junction region. In this equation σ, v_{th} and N_t are the trap capture cross section, the carrier thermal velocity and the trap density, respectively. W is the width of the depletion region and A is the junction area.

Eq.(1) was found to give a good description of the dark I-V data. The terms I_{01}, I_{02} and R_{sh} were obtained from a modified linear regression to the data following the treatment of [ref 5] and the values obtained in this manner are determined to about 15 %. In most cases, the shunt resistance term was found have a negligible contribution to the current compared to the contribution from the I_{01} and I_{02} terms.

Figure 3 shows dark I-V curves measured at several temperatures for a $Ga_{0.47}In_{0.53}As$ photodiode. These measurements were made over the temperature range 200 to 300 K. The solid lines are fits to Eq.(1) and the agreement can be seen to be good. The current is dominated by the diffusion term for this sample,and the slopes of the lines are essentially q/k_BT except at low voltages. The recombination current was found to be small. Most of the photodiodes studied displayed similar behavior and the absence of a significant recombination current implies that the diodes have few effective recombination centers prior to irradiation, as was confirmed by the DLTS measurements described below.

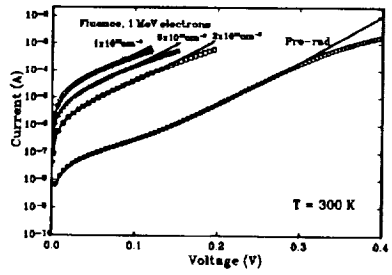

Figure 4: The effect of 1 MeV electron irradiation on the dark I-V characteristics of a $Ga_{0.47}In_{0.53}As$ photodetector.

The temperature dependence of the diffusion current was obtained from the fits, and an estimate for the gap energy was obtained from such data. The approximate T dependence of I_{01} is given by [ref 6]:

$$I_{01}(T) \sim n_i^2(T) \sim T^3 e^{-E_g/k_BT} \quad (4)$$

In Eq.(4), the weak temperature dependence of D_p and τ_p have been neglected. Inclusion of this would introduce only a few percent change, which is well within the present error bars [ref 7]. A value of 0.79 eV was obtained for E_g from fitting the data to Eq.(4). All of the photodiodes studied have been fitted in this fashion and the calculated E_g values range from 0.75 - 0.79 eV. Over the temperature range studied, the accepted band-gap value ranges from 0.75 eV to 0.78 eV [ref 8], in good agreement with the calculated values. Considering I_{01} is known to about 15%, this is further evidence of the good quality of these photodiodes prior to irradiation and lends credence to the use of Eq.(1) to describe the current.

Figure 4 shows the change in the room temperature dark I-V behavior due to irradiation with 1 MeV electrons. The dark I-V fits are shown as the solid lines and the description is reasonable for $I < 10^{-4}$ A. For $I > 10^{-4}$ A, the current tends to "roll-off" with increasing voltage. This most likely marks the onset of the high injection

region in which the minority carrier concentration becomes comparable to the majority carrier density. Rough calculations of the minority carrier density in this voltage range confirmed this to be the case. Since the junction is not well defined under these conditions, the dark I-V fits were made only for $I < 10^{-4}$ A. The "roll-of" for $I > 10^{-4}$ A might also be attributed to the series resistance of the sample; however, this does not appear to be the case since its inclusion did not describe the "roll-off" region well. Furthermore, the magnitude of the series resistance necessary to account for the "roll-off" would be so large that it would affect the current output throughout the entire voltage range which was not seen.

From the fits, I_{01} and I_{02} were determined following each incremental electron fluence. These values are listed in Table I. Figure 5 plots the recombination term vs. fluence. The data, although sparse, are consistent with I_{02} increasing linearly with fluence. In addition, it was determined that I_{01} (i.e. the diffusion current) dominated the diode current for voltages above ≈ 0.1 V throughout the fluence range studied.

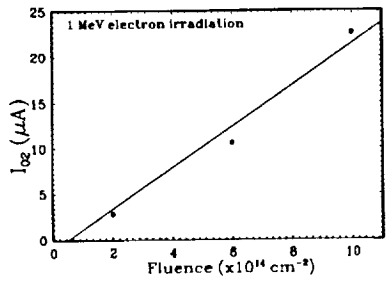

Figure 5: The increase in the recombination term, I_{02} due to 1 MeV electron irradiation. The solid line is a linear least square fit to the data.

B. Illuminated I-V Measurements

The response of the $Ga_{0.47}In_{0.53}As$ devices to 1 sun, AM0 illumination was characterized as a function of temperature and electron fluence. Figure 6 displays a typical photovoltaic (PV) I-V curve of the $Ga_{0.47}In_{0.53}As$ photodetectors measured at room temperature. Table II lists typical values of the PV parameters. The photodetectors appear to suffer from a series resistance which decreases the fill factor (FF). This is due to a lack of metal contact to the top of the sample. A photodetector is not critically dependent on the charge collection efficiency as is a solar cell; therefore, these devices have only a thin circle of metal surrounding the active region instead of a full metal grid of a solar cell. This is the major difference between these devices and a solar cell. Nevertheless, this difference will have no significant effect on the analysis of the radiation response of the $Ga_{0.47}In_{0.53}As$.

Table I
Calculated Dark I-V Parameters

$\phi \times 10^{14}$cm^{-2}	I_{01} (nA)	I_{02} (μA)
0	1.86	0.0209
2	558	2.76
6	2190	10.6
10	6000	22.6

Figure 7 displays the variation of the PV parameters of the photodetectors with temperature. The results are similar to those measured on InP homojunction cells [ref 9]. Since the variation of each parameter can be fit to a reasonably good straight line, the temperature coefficients were determined as the slope of the best fit line. The results are given in table III. V_{oc} follows the expected linear decrease with temperature, but the coefficient is less than 2 mV/K measured on InP and Si due to the smaller band-gap of $Ga_{0.47}In_{0.53}As$. The coefficient for J_{sc} is very similar to that of InP.

Figures 8 and 9 show the radiation-induced degradation of the PV response of the $Ga_{0.47}In_{0.53}As$ photodetectors. The data was measured at room temperature. All of the PV parameters show some degradation; however, figure 9 shows that V_{oc} is the parameter most affected. I_{sc}, on the other hand, shows only moderate degradation. Thus, it is the degradation in V_{oc} which is mainly responsible for the decrease in the cell output under irradiation.

The dark I-V parameters were used to predict the radiation-induced degradation of V_{oc}. V_{oc} can be calculated by the following expression [ref 10] where I_0 represents the dominant term between I_{01} and I_{02}:

$$V_{oc} = \frac{kT}{q} \ln \left(\frac{I_{sc}}{I_0} + 1 \right) \qquad (5)$$

The dark I-V data showed I_{01} to dominate in the voltage range near V_{oc}; therefore, V_{oc} was calculated from the

values of I_{sc} and I_{01}. The results of these calculations are shown in Table IV. It can be seen that the agreement of the predicted V_{oc} values and those measured is quite good.

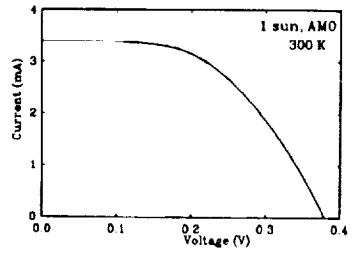

Figure 6: Typical IV curve for the $Ga_{0.47}In_{0.53}As$ photodetectors. The FF is low due to series resistance caused by lack of top metal contact to the photodetectors.

Table II
Typical Room Temperature $Ga_{0.47}In_{0.53}As$ PV Parameters

J_{sc} (mA/cm²)	48
V_{oc} (V)	0.379
FF	0.521
P_{max} (mW/cm²)	9.5
Eff (%)	6.9

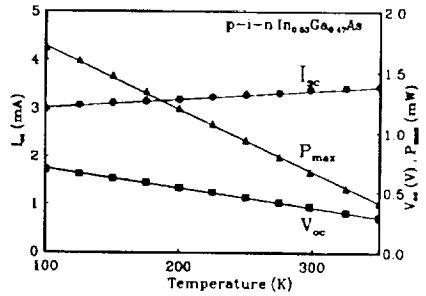

Figure 7: The effect of temperature on the PV parameters of a $Ga_{0.47}In_{0.53}As$ photodetector.

Table III
Temperature Coefficients for $Ga_{0.47}In_{0.53}As$

dI_{sc}/dT $\mu A/cm^2 \cdot K$	dV_{oc}/dT mV/K	dEff/dT %/K
25.6	1.65	0.055

C. DLTS Measurements

Before irradiation, no DLTS signal was detected. The DLTS spectrum measured after 1 MeV electron irradiation is shown in figure 10. The two radiation-induced peaks are majority carrier trapping centers and have been labeled E1 and E2 as shown. Despite extensive experiments to detect minority carrier trapping centers, none were found. The activation energy (E_a) and the capture cross-section obtained from the y-intercept of the Arrhenius plots (σ_∞) for E1 and E2 are given in Table 5. Since these centers capture electrons, E_a is measured from the conduction band as indicated in figure 10. At each fluence level, the defect concentration was estimated from the DLTS peak height by the usual approximation [ref 11]:

$$N_t = 2 \times \left(\frac{\Delta C}{C}\right) \times N_D \qquad (6)$$

where ΔC is the DLTS peak height, C is the quiescent capacitance, and N_D is the carrier concentration of the device. The introduction rate of E2 was found to be $0.07 \pm 0.01 cm^{-1}$.

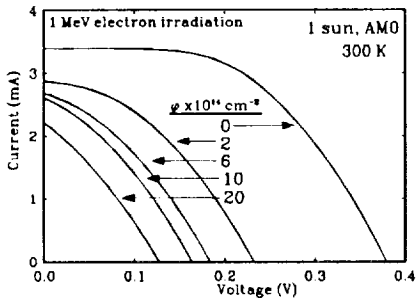

Figure 8: The degradation of the $Ga_{0.47}In_{0.53}As$ IV curves under 1 MeV electron irradiation.

Table IV
Prediction of V_{oc} From the Dark I-V Data

$\phi \times 10^{14}$ cm^{-2}	I_{01} (nA)	V_{oc}(V) pred.	V_{oc}(V) meas.
0	1.86	0.373	0.380
2	558	0.222	0.231
6	2190	0.184	0.186
10	6000	0.156	0.160

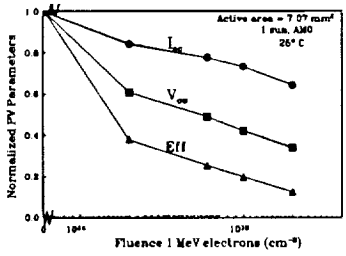

Figure 9: The degradation of the PV parameters. Normalized parameters are plotted to highlight that V_{oc} shows the most degradation while I_{sc} is only moderately degraded.

D. Annealing

An isochronal annealing experiment was performed on a photodiode after being irradiated with 2×10^{15} 1 MeV electrons cm^{-2}. The sample was held at elevated temperatures for 10 minutes at each temperature beginning at 325 K and increasing by 25 K at each step. The samples were annealed open circuit in the dark. The samples studied could not withstand temperatures above 450 K, so after 10 minutes at 450 K, the experiment was changed to isothermal annealing. The sample was then held at 450 K for three successive 30 min periods. This experiment was carried out in the liquid nitrogen cryostat of the DLTS system; therefore, it was not possible to measure the E1 defect during the annealing because the E1 peak occurs at too low of a temperature.

The results of the annealing experiment are presented in figure 11. Note that the abscissa of figure 11 breaks at 450 K from temperature to time. All PV parameters were measured at room temperature. The PV parameters are normalized to their pre-irradiation values while the E2 defect concentration is normalized to its maximum value. An annealing stage for the PV parameters is observed to begin at temperatures as low as 375 K. A large recovery in the PV parameters coinciding with a reduction in the E2 defect concentration occurs at 425 K. A further annealing stage is seen at 450 K. When the sample was held at 450 K for 90 minutes, the V_{oc} and maximum power appear to continue recovering while I_{sc} remains unchanged. The E2 defect concentration seems to follow an exponential decay as would be expected for a first order thermally activated annealing process; however, not enough data yet exists to draw any definitive conclusions about the annealing kinetics. It is also noteworthy that while significant recovery is seen in all the PV parameters, they are still far from full recovery even though the E2 defect concentration has decreased by nearly 90% after 90 minutes at 450 K.

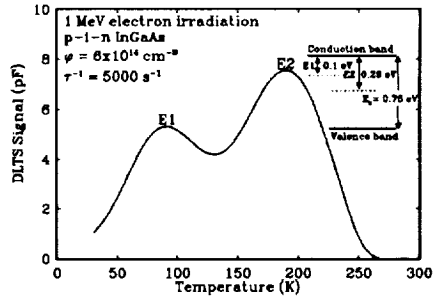

Figure 10: Typical DLTS spectrum measured on the $Ga_{0.47}In_{0.53}As$ material after 1 MeV electron irradiation.

Table V
Measured DLTS Parameters

	E_a eV	σ_∞ cm^2
E1	0.101	6.45×10^{-17}
E2	0.293	2.65×10^{-15}

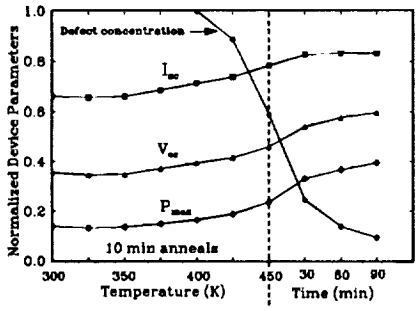

Figure 11: The results of thermally annealing an irradiated $Ga_{0.47}In_{0.53}As$ photodetector.

DISCUSSION

It is clear from the present study that 1 MeV electron irradiation decreases the photovoltaic response of the $Ga_{0.47}In_{0.53}As$ photodetectors by increasing the junction dark current. Since the dark current is most sensitive to defect levels nearest mid-band-gap, the increase is tentatively associated with the introduction of the E2 defect level. The increase in dark current was directly shown to decrease the PV response of the $Ga_{0.47}In_{0.53}As$ devices. Also, the recovery of the PV parameters during thermal annealing seems to be correlated with the decrease of the E2 defect concentration. Therefore, it seems that the E2 defect strongly controls the PV response of these $Ga_{0.47}In_{0.53}As$ photodetectors. Although the E1 defect concentration was not monitored during the annealing, it is not expected to have a large effect on the device performance since it is relatively far from mid-gap and thus will not be an efficient recombination center. Also, some of the experimental results obtained in this research suggests that E1 and E2 are caused by a single defect center, but this is still uncertain. From what is known about radiation-induced defects in GaAs, the most likely defect center which would give rise to this type of DLTS spectrum would be expected to be associated with an As vacancy. However, DLTS alone is not sufficient to determine the nature of the defect.

It is interesting to note that the V_{oc} of these devices is the parameter most degraded by irradiation. The increased sensitivity of V_{oc} can be explained in terms of the device structure. It was seen in InP homojunction cells that a decrease in the base dopant level caused a decrease in the radiation resistance of V_{oc} but an increase in the resistance of I_{sc} [ref 12,13]. This is thought to be due to the increase in W in the more lightly doped samples. With a wide depletion region, the radiation-induced defects are more likely to act as recombination centers and thus increase the recombination current and decrease V_{oc}. Also with a wide depletion layer, charge collection occurs more by drift through the depleted layer than by diffusion through the bulk. This makes charge collection in lightly doped samples very insensitive to changes in the minority carrier lifetime, thus I_{sc} is little affected by irradiation in such devices.

The present radiation degradation seems to fit this model. The samples are very lightly doped ($N_d \approx 4\times10^{15}$ cm^{-3}), and as they are irradiated, the recombination current increases which seems to be correlated with the introduction of the E2 defect. This increase was directly shown to decrease V_{oc}. However, I_{sc} is not degraded nearly as much as V_{oc}. The InP research also showed that by increasing the dopant level, the sensitivity of V_{oc} is decreased since less of the base region will be depleted. Since the present results show V_{oc} to be the major cause of the device degradation, a more heavily doped base seems to be in order to improve the radiation hardness.

By the converse of the arguments presented above, an increase in the dopant concentration, while decreasing the sensitivity of V_{oc} to irradiation, will increase the sensitivity of I_{sc}. This is an important consideration since the data indicates a significant degradation of I_{sc} even in the present device geometry. It was seen with the InP homojunctions that a decreased base thickness will offset this increased sensitivity of I_{sc}. A thinner base is also expected to increase the resistance of V_{oc}. Therefore, a more heavily doped, thinner $Ga_{0.47}In_{0.53}As$ bottom cell may be the most radiation resistant configuration for the tandem.

If the trend described above is generally evident in $Ga_{0.47}In_{0.53}As$ as it seems to be in InP, the result will be a tremendous flexibility in the design of the tandem cell. In particular, it would be expected that by adjusting the

base thicknesses and dopant levels of the component cells, the currents can be matched in the tandem, and moreover, the current can be made to be virtually insensitive to particle irradiation up to fluences of 10^{16} 1 MeV electrons cm^{-2}. However, it is stressed that these are currently only speculations. The next stage in the NRL research will be to irradiate $Ga_{0.47}In_{0.53}As$ solar cells of various dopant levels and thickness to determine the relative degradation rates of I_{sc} and V_{oc}.

CONCLUSIONS

This study has presented a preliminary characterization $Ga_{0.47}In_{0.53}As$ as a space solar cell material. The temperature coefficients of the PV parameters have been presented which follow the expected general trends. One MeV electron irradiation have been shown to introduce two majority charge carrier trapping centers, labeled E1 and E2, which have been characterized by DLTS. The preliminary indication is that the E2 defect causes an increase in the junction dark current which has been shown to decrease V_{oc}. It is the degradation of V_{oc} which dominates the degradation of the device output. The degradation seems to fit the model presented for InP solar cells, and a thinner, more heavily doped (i.e $N_a > 4\times10^{15}$ cm^{-3}) $Ga_{0.47}In_{0.53}As$ bottom cell is expected to show an increased radiation resistance. By also adjusting the structure of the InP top cell in a similar manner, a current matched, radiation resistant tandem solar cell with efficiencies >23% (AM0,1 sun) are realistically achievable.

REFERENCES

[1] M.W. Wanlass, J.S. Ward, T.J. Coutts, K.A. Emery, T.A. Gessert, and C.A. Osterwald. "Monolithic InP/$Ga_{0.47}In_{0.53}As$ Tandem Solar Cells for Space", Proc. of the Space Photovoltaic Research and Technology Conf., NASA Lewis Research Center, Cleveland Ohio, May 7-9, 1991. NASA Pub. #3121.

[2] M.W. Wanlass, J.S. Ward, T.J. Coutts, K.A. Emery, T.A. Gessert, and C.A. Osterwald. "Advanced High-Efficiency Concentrator Tandem Solar Cells", (Plenary paper) Proc. 22nd IEEE Photovoltaic Specialist Conf., Las Vegas, NV, Oct. 7-11, 1991.

[3] M.W. Wanlass, J.S. Ward, K.A. Emery, T.A. Gessert, C.A. Osterwald, and T.J. Coutts, "High-Performance Concentrator Tandem Solar Cells Based on IR-Sensitive Bottom Cells", Solar Cells, **30**, 363 (1991)

[4] R.J Walters, G.J. Shaw, G.P. Summers, M.W. Wanlass, and S.J. Ward, "Irradiation of Monolithic InP/$Ga_{0.47}In_{0.53}As$ Tandem Solar Cells", Fourth International Conf. on InP and Related Materials, April 21-24, Newport, RI. 1992

[5] G.L. Araujo, E. Sanchez and M. Marti, Solar Cells, 5 (1982) 1990

[6] S.M. Sze, Physics of Semiconductor Devices, (Wiley, New York,1981).

[7] T.P. Pearsall, G. Beuchet, J.P. Hirtz, N. Visentin, and M. Bonnet, "Electron and Hole Mobilities in $Ga_{0.47}In_{0.53}As$". Gallium Arsenide and Related Compounds Vienna, 1980 (Bristol, Inst. of Phys.) 639-649

[8] S.R. Forrest, R.F. Leheny, R.E. Nahory, and M.A. Pollack, "$Ga_{0.47}In_{0.53}As$ Photodiodes With Dark Current Limited by Generation-Recombination and Tunneling", Appl. Phys. Lett., **37**, 322, Aug. 1980

[9] R.J. Walters, R.L. Statler, and G.P. Summers, "Temperature Coefficients and Radiation Induced DLTS Spectra of MOCVD Grown n^+p InP Solar Cells", Proceedings of the Space Photovoltaic Research and Technology, NASA Conference Publication 3121, NASA Lewis Research Center, Cleveland, Ohio May 7-9, 1991.

[10] M.A. Green, Solar Cells: Operating Principles, Technology, and System Applications, (Prentice Hall, Englewood Cliffs: New Jersey, 1982)

[11] D.V. Lang. "Fast Capacitance Transient Apparatus: Application to ZnO and O centers in GaP p-n junctions", J. Appl. Phys., **45**, 3014, July 1974

[12] R.J. Walters, C.J. Keavney, S.R. Messenger, G.P. Summers, and E.A. Burke, "The Effect of Dopant Density on the Radiation Resistance of MOCVD InP Solar Cells", Proceedings of the Photovoltaic Specialists Conference, Las Vegas, NV, October 1991.

[13] C.J. Keavney, R.J. Walters, and P.J. Drevinsky, "Optimizing the Radiation Resistance of InP Solar Cells: The Effect of Dopant Density and Cell Thickness", J. Appl. Phys., **73**, Jan. 1 (1993)